РОССИЙСКИЙ ФИЗИОЛОГИЧЕСКИЙ ЖУРНАЛ им. И.М. СЕЧЕНОВА 2020, том 106, № 9, с. 1098–1108

ЭКСПЕРИМЕНТАЛЬНЫЕ СТАТЬИ

EVALUATION OF THE T-SYSTEM OF RAT CARDIOMYOCYTES DURING EARLY STAGES OF STREPTOZOTOCIN-INDUCED DIABETES

© 2020 I. V. Kubasov[1], D. E. Bobkov[2], A. V. Stepanov[1], I. B. Sukhov[1], O. V. Chistyakova[1], and M. G. Dobretsov[1, *]

[1]*Sechenov Institute of Evolutionary Physiology and Biochemistry, Russian Academy of Sciences, St. Petersburg, Russia*

[2]*Institute of Cytology, Russian Academy of Sciences, St. Petersburg, Russia*

**e-mail: dobretsovmaxim@gmail.com*

Received April 27, 2019
Revised June 15, 2020
Accepted July 10, 2020

Disorganization of the T-system of cardiomyocytes is considered an early and critical step in the development of Diabetic Cardiomyopathy (DCM). To test this suggestion, male Wistar rats were injected with streptozotocin (STZ, 30 or 45 mg/kg) and studied one month later. STZ-rats that developed and maintained hyperglycemia (random blood glucose >11 mM) were designated as hyperglycemic (STZ-HG) rats, while the remaining STZ-rats – as normoglycemic (STZ-NG) animals. The structural integrity of the T-system was investigated using an analysis of confocal images of the left ventricle (LV) sub-epicardium of isolated hearts, stained with the Di-8-ANEPPS. In control, T-system was organized into regular networks of t-tubules aligned with Z-discs of cardiomyocyte's sarcomeres. Accordingly, the frequency distributions of intervals between neighboring t-tubules (INT, measured along the major cell axis) peaked at a 2 μm value with not more than 21% of INT (per cell) exceeding the 3 μm cut-off. Only 4 ± 3% of the control cardiomyocytes (274 cells, 4 rats) could be considered as deficient, according to this parameter (>21% occurrence of long INT). Compared to control, in the hearts of STZ-NG and STZ-HG rats, the fractions of such deficient cardiomyocytes were statistically significantly higher: 48 ± 13% (STZ-NG, 8 rats, 573 cells) and 76 ± 8% (STZ-HG, 4 rats, 247 cells). Thus, structural changes in the T-system of the rat heart LV cardiomyocytes develop early during chronic hyperglycemia (overt diabetes) as well as during near-normoglycemic stages of diabetes (prediabetes). The relevance of these changes to the development of DCM in subjects with prediabetes remains to be studied.

Keywords: cardiomyocyte, cardiomyopathy, confocal microscopy, Diabetes Mellitus, hyperglycemia, T-system, rat

DOI: 10.31857/S0869813920090046

Diabetic cardiomyopathy (DCM) is one of the most common complications of Diabetes Mellitus (DM). DCM equally affects patients with Type I and Type II DM (T1DM, insulin-dependent and T2DM, insulin-independent DM, respectively) leading on its terminal stages to cardiac failure (CF) and thus constituting the major reason of mortality in this patient population. Despite the gravity of this disease, the etiology of DCM remains poorly

Abbreviations: DCM – diabetic cardiomyopathy; INT – intervals between neighboring t-tubules; LV – left ventricle; ROI – region of interest, STZ – streptozotocin; STZ-HG – hyperglycemic STZ-injected rats; STZ-NG – normoglycemic STZ-injected rats; T1DM / T2DM – type I / type II Diabetes Mellitus.

understood [1]. In particular, DCM is diagnosed when symptoms and clinical signs of the left ventricle hypertrophy and dysfunction are present on a background of DM (chronic hyperglycemia, fasting blood glucose >7 mM or random glucose >11 mM) and in the absence of hypertonia or signs of macrovascular disease [2, 3]. An almost inevitable byproduct of this definition of DCM is the view of chronic hyperglycemia as the major, if not the only, trigger of the pathogenesis of DCM [1, 3]. The hyperglycemic hypothesis of DCM, however, clearly conflicts with accumulating evidence of the abnormally high risk of development of left ventricle hypotrophy and dysfunction observed in populations of human and animal subjects with border side hyperglycemia characterizing states of prediabetes or well-controlled DM [4–10]. These latter observations raise the question about the need for more detailed structure-functional cardiac studies conducted on early stages of DM when insulin deficiency (T1DM) or insulin resistance (T2DM) have not yet translated into substantiating changes in glucose and fat metabolism (early prediabetes). The inquiry into the time of onset of deterioration/remodeling of the T-system of cardiomyocytes appears to be particularly significant. The T-system or the highly structured network of transverse invaginations (t-tubules) of ventricular cardiomyocyte plasma membrane inside the cell plays a critical role in the control of electromechanical coupling and cardiomyocyte contractility [11]. In various animal models of CF structural reorganization of T-system consisting of a decrease in t-tubular density, their dilatation and impairment in their alignment with Z-discs of myocyte sarcomeres are observed long before signs of CF become apparent [12, 13]. Similar changes in the structural integrity of T-system develop and closely coincide with myocardial functional impairment in the hearts of rodents on advanced stages (8 or more weeks) of experimental T1DM and T2DM [14–18]. However, we found no references to the work evaluating the T-system of cardiomyocytes at early terms of acute DM or on prediabetic stages of the disease. As a first step to address this issue, in the current work, the integrity of T-system of left ventricle cardiomyocytes was studied in rats with short-term (4 weeks) streptozotocin (STZ)-induced chronic hyperglycemia and in rats that after injection of pancreatic toxin STZ remained normoglycemic or developed moderate and transient hyperglycemia only. The first group of rats constitutes a well-established model of acute T1DM in which early (1–4 weeks) deterioration in ventricular cardiomyocyte electrogenesis and contractility was universally documented [19–23]. The second group of animals, when studied at 2 weeks, was shown mimicking the early prediabetic state of the disease [24].

RESEARCH METHODS

A total of 16 male Wistar rats (age 3 months, weight 250–350 g) were used in experiments. Animals were kept in standard vivarium conditions (6 rats per cage) at 22°C and relative air humidity of 50–65%. During experiments, rats had free access to water and food. All applicable international, national, and institutional principles of handling and using experimental animals for scientific purposes were observed.

At the beginning of the experiment, 12 rats randomly selected from a total pool were injected intraperitoneally with pancreatic toxin streptozotocin (STZ, Sigma-Aldrich, USA) at a dose of 30 and 45 mg/kg (8 and 4 rats, respectively). The remaining 4 rats were injected with an equivalent volume of the vehicle solution (control, 0.1 M Na-citrate buffer, pH 4.5; 0.1 mL/100 g body weight). The random blood glucose (RG) levels of experimental animals were measured on days 3, 14, and 28 of the experiment using tail capillary blood samples, One Touch Ultra test strips (USA), and Life Scan Johnson & Johnson glucometer.

On the last day of the experiment, the animals were deeply anesthetized with chloralhydrate (400 mg/kg, intraperitoneally; Merck, Germany), their hearts were removed and mounted on a Langendorff apparatus for retrograde perfusion with aerated Tyrode solution containing (mM): NaCl 140, KCl 4.5, $CaCl_2$ 1, $MgCl_2$ 1, HEPES 10, glucose 10, pH 7.2–7.4.

2,3-Butanedione monoxime (20 mM, Sigma-Aldrich, USA) and fluorescent dye Di-8-ANEPPS (20 μM; Thermo Fisher Scientific, USA) were added to the perfusing solution to, respectively, block myosin ATPase, suppress heart contractility, and to stain the plasma membrane of the cells of the myocardium [25, 26].

Cardiomyocytes of the left ventricle heart sub-epicardium were studied using the TCS SP5 MP confocal microscope, equipped with an 8000 Hz resonance scanner and 20×–60× objectives (NA = 1.3; Leica, Wetzlar, Germany). The isolated heart was placed left ventricle down (toward the objective) into the 180 μm-thick glass bottom μ-dish (IBIDI GmbH, Planegg, Germany). The sample was illuminated using an argon laser (488 nm wavelength; 80% power), which emitted a fluorescent signal that was recorded within 600–690 nm spectral range at the pinhole setting of 100 μm. For each heart, 7 to 15 images (205 × 205 μm, 5 pixels/μm) were captured within randomly selected fields of the first epicardial layer fields at the confocal depth of about 10–15 μm from the surface of the myocardium.

Image analysis was conducted using Fiji – ImageJ freeware (NIH, USA). To determine the cardiomyocyte physical dimensions, each cardiomyocyte within the borders of the image was outlined with a Polygon Selection tool. The area of this polygon ROI and lengths of minor and major axes of the ellipse's best fit to the ROI were measured as, respectively, area, width, and length of the myocyte. To estimate the structural integrity of T-system of cardiomyocytes, each of captured images was sharpened (Fig. 1*A,* a) and processed with the Find Maxima algorithm to generate a black and white mask of the original image, in which each confocal cross-section of each t-tubule was reduced to a corresponding by location dark pixel (Fig. 1*A*, b). These mask images were then used to determine frequency distributions of intervals between neighboring t-tubules (INT, measured along the major cell axis). For each myocyte, a linear region of interest (ROI, line thickness = 5 pixels or 1 μm) was selected running along the major cell axis at about mid-width of the myocyte, but avoiding t-tubule free cell nuclei locations (Fig. 1*A*, a, b). Then the plot profile of this linear ROI was built, in which each intensity peak X-coordinate represents the X position of its corresponding t-tubule within given linear ROI (compare Fig. 1*A*, b and Fig. 1*B*, numbered arrows). Based on numerical data for such ROI plot profiles, INT were measured (custom Excel Visual Basic macro) and frequency distributions of INT were built for each studied cell (Fig. 1*C*, a), with subsequent averaging to obtain integral INT frequency distri-

Fig. 1. Analysis of structural integrity of T-system of left ventricle cardiomyocytes in confocal sections of Di-8-ANEPPS-stained rat heart.

A. Representative image of a control rat heart cardiomyocyte before (A, a) and after (A, b – binary mask) application of Find Maxima ImageJ algorithm. Dark pixels in A, b represent detected t-tubular profiles. Line (semitransparent in A, b) shows 5-pixels-thick longitudinal ROI selected at the cell mid-width, but to avoid t-tubule-free cell nuclei regions (text labels "n").

B. The plot profile obtained for the ROI shown in A. Profile Y value corresponds to the average intensity of all pixels across the ROI at given X value of the ROI.

C. Subpanel "a" – Frequency distribution of INT calculated for the cell and ROI shown in panels A and B. In correspondence with the sarcomeric arrangement of the T-system, most of INT measured are distributed around 2 μm value (main peak). However, there is also substantial for a given cell and ROI fraction of short intervals (asterisk), representative of profile regions containing misaligned t-tubules. Two of such regions are outlined by ovals and marked by asterisks in A and B panels. There are also profile regions with INT exceeding 3 μm (vertical dashed line) in length. Comparison of the figure panels A–C shows that appearance of such long INT is associated with the appearance of gaps in the regular sarcomeric organization of t-tubules (see arrows "1a-c" and "3" marking segments of ROI and its plot profile, where, respectively, one or three in row t-tubules are missed at their expected location). Subpanel "b" – Average INT distribution (same control rat as above, 8 fields, 48 cardiomyocytes). The smooth solid line represents the result of the best fit to the distribution of two Gaussian curves. Some of the fit or derived from the fit parameters are shown next to the marking of the respective peak arrows.

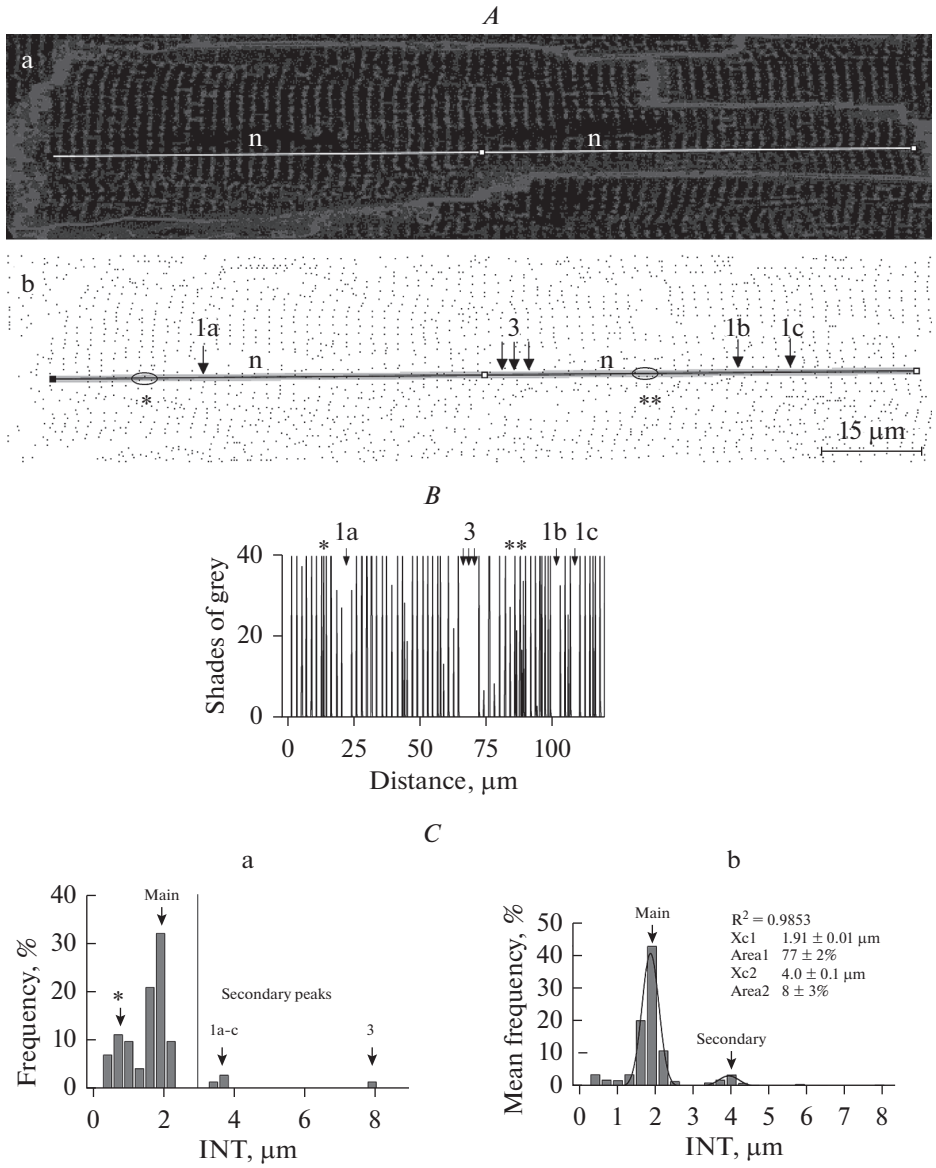

butions characterizing all cells studied within the given image (Fig. 1*C*, b) or given rat heart. Individual cardiomyocyte INT distributions were used to determine the fraction of long, exceeding an arbitrary value of 3 μm INT (Fig. 1*C*, a, vertical dashed line), and averaged INT distributions were used to determine the parameters of their primary and secondary peaks. For the latter, the best fit procedure of INT distributions with two or three (as appropriate) independent Gaussian curves were employed (Fig. 1*C*, b; Origin 6.0, OriginLab, Northampton, Massachusetts, USA).

Prizm 4.5 (Graphpad Software Inc., San Diego, California, USA) software was used for statistical data analysis. Sample means were compared assuming normal data distri-

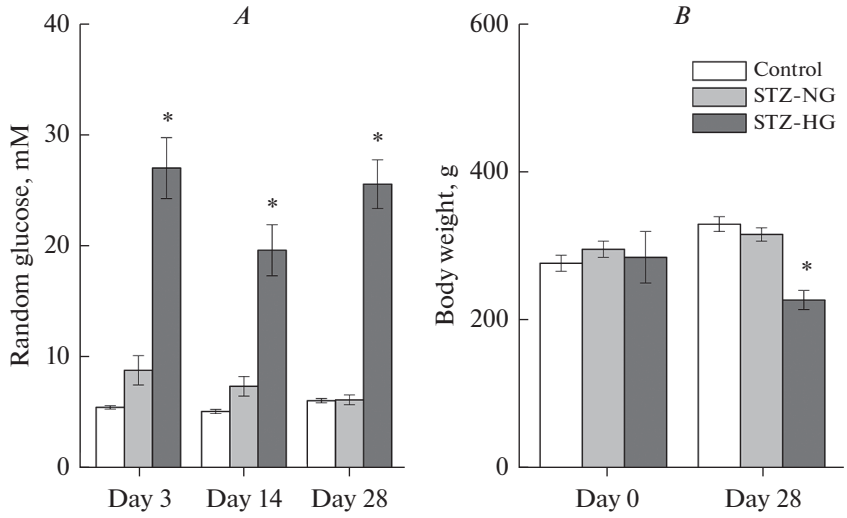

Fig. 2. Random blood glucose (*A*) and weight (*B*) of experimental animals on different days of the experiment before (day 0) and after STZ injection (Mean ± SEM). Asterisks indicate a statistically significant difference between the given group and other groups' mean values ($p < 0.05$; comparisons for the selected day of the experiment).

bution using one- and two-way ANOVA followed by, respectively, Tukey and Bonferroni tests for multiple comparisons. Mean values were considered to be significantly different at p-value < 0.05.

RESEARH RESULTS

At the beginning of the experiment, the RG of animals was in the range of 5 to 6 mM (mean RG0 = 5.4 ± 0.1 mM; $n = 16$). Control group rats maintained this level of RG throughout the entire experiment. All 4 rats injected with 45 mg/kg STZ developed chronic diabetes. Their RG level exceeded the accepted in this work 11.1 mM diabetes definition threshold during all three tests (days 3, 14, and 28). These rats were designated as STZ-HG group rats. Of 8 animals that received 30 mg/kg STZ, one rat remained normoglycemic throughout the rest of the experiment, one developed acute, but transient diabetes (RG3 = 17.6), and the remaining 6 rats developed transient intermediate hyperglycemia (RG3 = 7–10 mM). Since on the last day of the experiment all of these animals maintained normoglycemia, they were assigned to the STZ-NG group. Mean RG levels of STZ-HG rats were significantly higher, compared to those measured for the same time points in control. However, by this parameter, the STZ-NG rats demonstrated no statistically significant difference from the control at any of the three studied time points (Fig. 2*A*). Weights of the control, STZ-NG, and STZ-HG rats did not differ at the beginning of the experiment. By the end of the experiment, the weight of STZ-HG, but not of STZ-NG rats, was significantly lower than that of the control animals (Fig. 2*B*).

Such indexes of cardiac/ventricular hypertrophy/atrophy as relative heart weight or measurements of cardiac myocyte area, length of width had not revealed any significant differences between studied groups of rats (Table 1).

In sharp contrast with the stability of the indexes above, compared to control (Figs. 1*B*, b and 3*B*, a), confocal sections of a subepicardial myocardium of LV of STZ-NG rats and even more frequently of STZ-HG (Figs. 3*A*, b and 3*A*, c) contained cardiomyocytes demonstrating signs of impairment of normally regular sarcomeric organization of T-sys-

Table 1. Indexes of cardiac/ventricular hypertrophy/atrophy (Mean ± SEM)

Index	Control ($n = 4$)	STZ-NG ($n = 8$)	STZ-HG ($n = 4$)
	Heart		
Weight, g/100g body weight	0.45 ± 0.03	0.47 ± 0.03	0.51 ± 0.06
	Cardiomyocyte		
Length, μm	114 ± 5	114 ± 4	116 ± 7
Width, μm	21 ± 1	22.1 ± 0.7	21.5 ± 0.9
Area, μm^2	1864 ± 152	1979 ± 61	1975 ± 82

tem. This impairment manifested itself in a decreased density of detectable t-tubular profiles, which, in some of the myocytes of STZ-HG rats, produced a picture of "moth-eaten" damage to a normally regular network of t-tubular profiles (Fig. 3*A*, c). Analysis of longitudinal INT frequency distributions has confirmed these differences by demonstrating an increased, compared to control, number and height of secondary peaks in INT distributions of STZ-NG and STZ-HG rats (Figs. 3*B*, a–c and 3*C*, a). The total fraction of cardiac myocytes with abnormally long INT was also increased above that in control in the hearts of STZ-NG and STZ-HG rats (Fig. 3*C*, b, c). Abnormally long INT was defined in this study as INT exceeding 3 μm – valley separating primary and secondary peaks in INT distributions. In control hearts, an average myocyte had 9% of its INTs abnormal, according to this criterion. Respectively, cells with a deficient T-system were defined as cells in which the fraction of abnormal INT is higher than 21% (mean + 2SD; Fig. 3*C*, b). Only 4 ± 3% of the control heart cardiomyocytes (274 cells, 4 rats) could be considered as deficient, according to this definition. However, in the hearts of STZ-NG and STZ-HG rats, the fractions of such cardiomyocytes were statistically significantly higher than those in control (Fig. 3*C*, c): 48 ± 13% (STZ-NG, 8 rats, 573 cells) and 76 ± 8% (STZ-HG, 4 rats, 247 cells).

DISCUSSION

In various animal models of cardiac failure structural reorganization of T-system consisting of a decrease in t-tubular density, their dilatation and misalignment with sarcomeric Z-discs start before signs of CF become apparent [12, 13]. Changes in the structural integrity of the T-system also develop in the hearts of rodents on advanced stages (8 or more weeks) of experimental DM [14–17]. The major finding of our study consists of providing evidence of the early beginning of the reorganization of T-system in rats with STZ-induced T1DM – 4 weeks of chronic hyperglycemia. Furthermore, first-time evidence was provided that t-tubular remodeling may be detected in the left ventricle myocytes of hearts of rats that, after injection with STZ, developed transient or no hyperglycemia at all. This latter finding suggests the possibility of hyperglycemia-independent structural changes in the myocardium, which may change our understanding of the pathogenesis of DCM in subjects with prediabetes.

STZ-HG rats

These rats represent the classical model of acute insulin-dependent DM [24]. As expected for such animals, they developed and maintained severe hyperglycemia and displayed a net weight loss (Fig. 2). We found no signs of gross morphological heart abnormalities, such as changes in heart/body weight index or myocyte width or length (Table 1), which might be because of the short-term (4 weeks) the disease state was studied in our work [17, 19, 23]. Even at this early term, confocal image analysis demonstrated clear signs

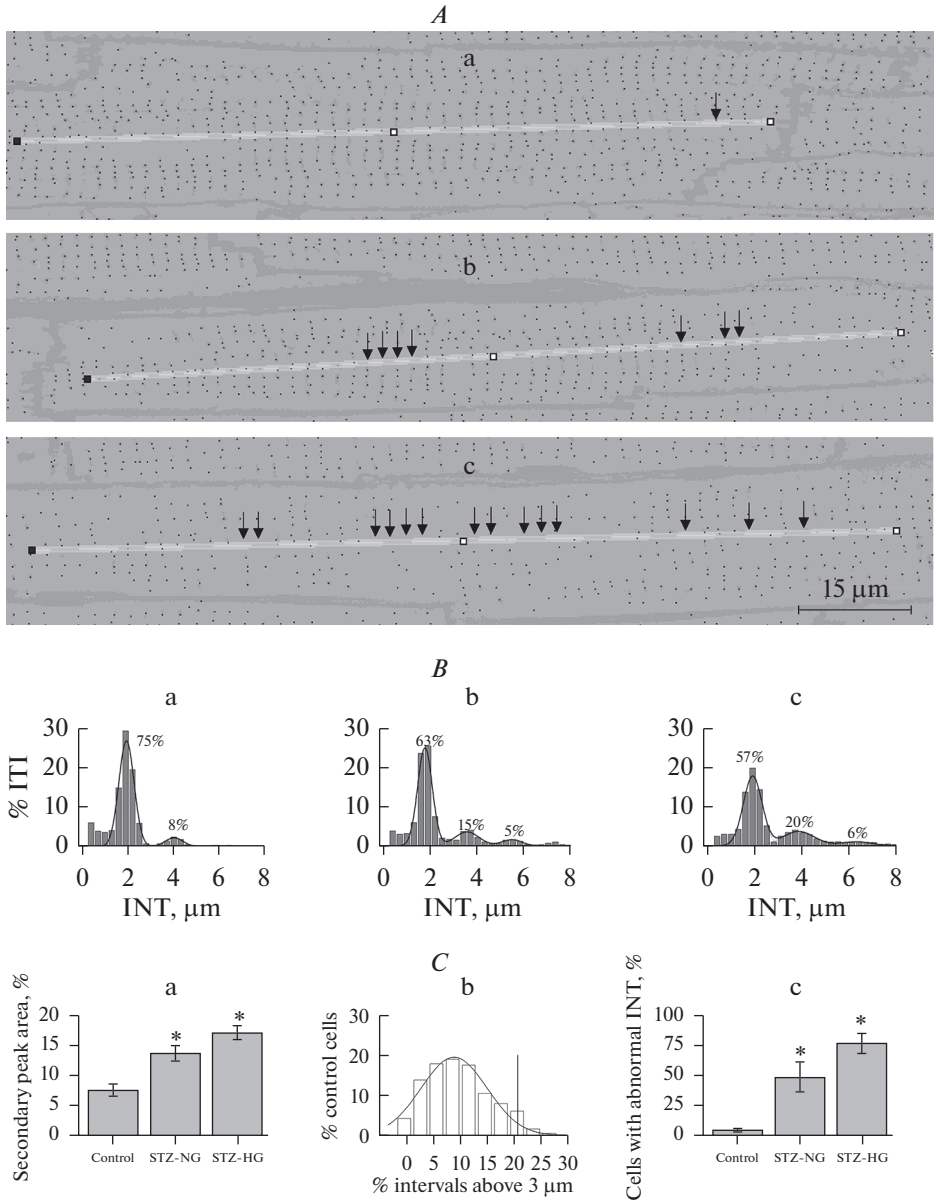

of disorganization of the LV cardiomyocyte T-system. Thus, in control (Figs. 1 and 3), the major peak in INT distributions was found at 2 μm, which is well within the range of 1.7–2.2 μm reported for rat cardiomyocyte sarcomere length and consistent with the fact that normally t-tubules are arranged in the regular networks aligned with Z-discs of mammalian myocyte sarcomeres [17, 27]. There was also a secondary peak at about 4 μm (~8% of INT), suggesting the existence of a small fraction of sarcomeres missing any t-tubule over 1 μm (selected ROI width) cross-sectional profile. On average, no more than 21% (mean + 2 SD) of control myocytes were deficient in this regard. Compared to control, INT distributions of

Fig. 3. The regularity of the T-system of left ventricle cardiomyocytes of control, STZ-NG, and STZ-HG rats.
A. – Representative examples confocal sections of control, STZ-NG, and STZ-HG rat myocytes (sub-panels a, b, and c, respectively) overplayed with black and white masks of the same images processed to detect cross-sectional t-tubular profile (black dots). Yellow, 5-pixel in width lines are ROI selection lines used to determine the regularity of sarcomeric alignment of the t-tubular network. Arrows point to the ROI segments with one or more (number of arrows) sequential sarcomeres lacking expected t-tubule profile.
B. – Average INT distributions of control, STZ-NG, and STZ-HG rat myocytes (sub-panels a, b, and c, respectively). Shown in plots, solid smooth lines are a result of the best fit to the distribution of two or three Gaussian curves. Number next to the peak indicates the percentage of INT belonging to the respective peak in the distribution calculated from the best fit procedure parameter results.
C. – Analysis of a degree of irregularity in longitudinal T-system organization. Sub-panel "a" shows the first secondary peak areas (group mean ± SEM; based on results of the multi-Gaussian best-fit procedure, see panel B). This parameter describes the occurrence of stand-along sarcomeres missing corresponding t-tubule profile (panel A, single arrow). Sub-panel "b" shows the frequency distribution of the control hearts LV myocytes according to their INT right-hand tail area. This graph shows that most of the cells in control (96%, mean + 2SD, vertical dashed line) have >21% occurrence of long INT according to this parameter. Sub-panel "c" shows the group means (±SEM) of frequencies of cells deficient in this parameter in the hearts of control, STZ-NG, and STZ-HG rats. Asterisks indicate a statistically significant difference ($p < 0.05$) between the given group and control group mean values.

cardiomyocytes of STZ-HG rats were different, demonstrating a prominent right-hand tail composed of two or more secondary peaks. X values of these secondary peaks appeared as multiples of X value of the major peak of respective INT distribution (see, for example, Fig. 3*B*, c: 2.0, 3.9 and 6.3 μm – X values for the main and first and second secondary peaks, respectively), which may be interpreted as an increase in the occurrence of situations when 1, 2, 3, etc. consecutive sarcomeres have corresponding t-tubule missing. This phenomenon may be attributed to the sealing-off and vesiculation of some segments of t-tubules, leading to an inability of membrane-impermeable dyes to reach and stain the membrane of these t-tubular vesicles, which is observed during osmotic detubulation of cardiac myocytes [28, 29]. Alternatively or in addition to the mechanism above, structural disorganization, consisting in a loss of the uniform, transverse T-tubule pattern, with a higher proportion of tubules present in the longitudinal direction may also explain the observed increase in the fraction of "t-tubule-depleted" sarcomeres in myocytes of diabetic rats [12]. Integrity and regularity of T-system is a critical condition ensuring depolarization of myocyte by an action potential, the synchronicity of calcium-induced calcium release and the cell contractility [11]. Therefore, regardless of the exact mechanisms of early disorganization of the T-system of STZ-HG rat cardiomyocytes observed in our work, this disorganization undoubtedly contributes to the pathogenesis of impaired contractility of cardiomyocytes isolated from hearts of STZ-diabetic rats [11, 17].

STZ-NG rats

Rats classified in this work as STZ-NG rats developed no chronic, but transient hyperglycemia or remained normoglycemic after STZ injection. Previously, it was shown that in the second week of the experiment, STZ-NG rats are moderately insulinopenic and thus mimic the state of early insulin-dependent prediabetes. However, during the subsequent two weeks (by a total 4-week term), putatively due to the regeneration of insulin-producing β-cells, these animals recover to the normal insulin level [30]. A similar dynamic in pancreatic injury and insulin production might well explain transient RG changes observed for STZ-NG rats in our study (Fig. 2). If this suggestion were confirmed, we would need to conclude that even a short-lived prediabetic state may leave a lasting imprint on the structural organization of rat heart LV myocyte T-system.

Indeed, deficiency of the T-system of cardiomyocytes of 4-week STZ-NG rats was revealed in this study by both measured parameters: area of the first secondary peak in INT distribution and % of cells with the above-threshold occurrence of abnormally long INT (Fig. 3).

Possible mechanisms of T-system injury

Chronic hyperglycemia is considered as a trigger for all major, including DCM, complications of DM [18]. Our finding of a decrease in t-tubular density in rats from the STZ-NG group is, however, challenging this view, suggesting instead that factors other than overt chronic hyperglycemia are likely to be responsible for the observed phenomena.

The direct toxic effect of STZ on rodent heart cardiomyocytes cannot be ruled out but seems to be very unlikely for at least two reasons. First, selective toxicity of STZ toward pancreatic beta cells is explained by intracellular uptake STZ via GLUT2 isoform of the glucose transporter [31]. Rat cardiomyocytes, however, do not express this isoform of glucose transporter [32]. Second, functional as well as structural cardiac consequences of STZ-injection can be prevented or corrected by insulin therapy [2, 18].

Previously, two weeks-STZ-NG rats were introduced as a model of early prediabetes, in which the progression of selected signs of diabetic neuropathy (deep muscle and visceral evoked pains) was directly attributed to moderate insulinopenia. In particular, it was suggested that regulation of systemic blood glucose and fat metabolism and regulation of pain control pathways might have different requirements in the maintained activity of insulin-controlled cellular pathways [24, 30, 33]. A tentatively similar explanation may be applied to the case of the integrity of the T-tubular system in the hearts of prediabetic and overtly diabetic subjects. However, to accept this explanation, we need to suggest that transient hyperglycemia and/or insulinopenia may have a relatively long-term effect on the structural integrity of the T-system of LV cardiomyocytes.

Therefore, further studies in animal models of diabetes and prediabetes, employing both the battery of glucose metabolism tests (random and fasting glucose measurements and glucose tolerance test) and plasma insulin measurements are needed.

FUNDING

This work was supported by Russian Foundation for Basic Research, award № 19-015-00139, and by Institute of Evolutionary Biochemistry and Physiology, Russian Academy of Sciences Government basic research program № 075-00776-19-02. The confocal microscope Leica TCS SP5 MP was provided by the Research Resource Center (Sechenov Institute of Evolutionary Physiology and Biochemistry, RAS).

ACKNOWLEDGMENTS

We thank Ms. Tatiana Dobretsova for her help with editing this manuscript.

AUTOR CONTRIBUTIONS

I.V. Kubasov – this author contributed to the study design and participated in confocal microscopy experiments and the manuscript editing. D.E. Bobkov – this author conducted confocal imaging experiments and participated in the data analysis and manuscript editing. A.V. Stepanov – this author helped conducting experiments, data analysis and manuscript writing. I.B. Sukhov and O.V. Chistyakova – these authors contributed equally to the rat model development and monitoring, data discussion and manuscript editing and preparation for submission. M.G. Dobretsov is the principle investigator in this study who contributed to the study design, the data analysis, discussion and interpretation, and the drafting and preparation of the final version of the manuscript.

REFERENCES

1. *Riehle C., Bauersachs J.* Of mice and men: models and mechanisms of diabetic cardiomyopathy. Basic Res. Cardiol. 114(2): 2. 2019.
2. *Dubo S., Gallegos D., Cabrera L., Sobrevia L., Zuniga L., González M.* Cardiovascular Action of Insulin in Health and Disease: Endothelial L-arginine transport and cardiac voltage-dependent potassium channels. Front. Physiol. 7: 74. 2016.
3. *Singh R. M., Waqar T., Howarth F. C., Adeghate E., Bidasee K., Singh J.* Hyperglycemia-induced cardiac contractile dysfunction in the diabetic heart. Heart Fail. Rev. 23: 37–54. 2018.
4. *Celentano A., Vaccaro O., Tammaro P., Galderisi M., Crivaro M., Oliviero M., Imperatore G., Palmieri V., Iovino V., Riccardi G., de Divitiis O.* Early abnormalities of cardiac function in non-insulin-dependent diabetes mellitus and impaired glucose tolerance. Am. J. Cardiol. 76: 1173–1176. 1995.
5. *Ren J., Sowers J.R., Walsh M.F., Brown R.A.* Reduced contractile response to insulin and IGF-I in ventricular myocytes from genetically obese Zucker rats. Am. J. Physiol. Heart Circ. Physiol. 279: H1708–H1714. 2000.
6. *Castagno D., Baird-Gunning J., Jhund P.S., Biondi-Zoccai G., MacDonald M.R., Petrie M.C., Gaita F., McMurray J.J.* Intensive glycemic control has no impact on the risk of heart failure in type 2 diabetic patients: evidence from a 37,229 patient meta-analysis. Am. Heart J. 162: 938–948. 2011.
7. *Grundy S.M.* Pre-diabetes, metabolic syndrome, and cardiovascular risk. J. Am. Coll. Cardiol. 59: 635–643. 2012.
8. *Nunes S., Soares E., Fernandes J., Viana S., Carvalho E., Pereira F.C., Reis F.* Early cardiac changes in a rat model of prediabetes: Brain natriuretic peptide overexpression seems to be the best marker. Cardiovasc. Diabetol. 12: 1–11. 2013.
9. *Tadic M., Celic V., Cuspidi C., Ilic S., Pencic B., Radojkovic J., Ivanovic B., Stanisavljevic D., Kocabay G., Marjanovic T.* Right heart mechanics in untreated normotensive patients with prediabetes and type 2 diabetes mellitus: A two- and three-dimensional echocardiographic study. J. Am. Soc. Echocardiogr. 28(3): 317–327. 2015.
10. *Huang Y., Cai X., Mai W., Li M., Hu Y.* Association between prediabetes and risk of cardiovascular disease and all-cause mortality: systematic review and meta-analysis. Br. Med. J. 355: i5953. 2016.
11. *Ibrahim M., Gorelik J., Yacoub M.H. Terracciano C.M.* The structure and function of cardiac t-tubules in health and disease. Proc. Biol. Sci. 278: 2714–2723. 2011.
12. *Louch W.E., Sejersted O.M., Swift F.* There goes the neighborhood: pathological alterations in t-tubule morphology and consequences for cardiomyocyte Ca^{2+} handling. J. Biomed. Biotechnol. 2010: 503906. 2010.
13. *Crossman D.J., Jayasinghe I.D., Soeller C.* Transverse tubule remodelling: a cellular pathology driven by both sides of the plasmalemma? Biophys. Rev. 9: 919–929. 2017.
14. *McGrath K.F., Yuki A., Manaka Y., Tamaki H., Saito K., Takekura H.* Morphological characteristics of cardiac calcium release units in animals with metabolic and circulatory disorders. J. Muscle Res. Cell Motil. 30: 225–331. 2009.
15. *Stølen T.O., Høydal M.A., Kemi O.J., Catalucci D., Ceci M., Aasum E., Larsen T., Rolim N., Condorelli G., Smith G.L., Wisløff U.* Interval training normalizes cardiomyocyte function, diastolic Ca^{2+} control, and SR Ca^{2+} release synchronicity in a mouse model of diabetic cardiomyopathy. Circ. Res. 105: 527–536. 2009.
16. *Cagalinec M., Waczulíková I., Uličná O., Chorvat D.* Morphology and contractility of cardiac myocytes in early stages of streptozotocin-induced diabetes mellitus in rats. Physiol. Res. 62: 489–501. 2013.
17. *Ward M.L., Crossman D.J.* Mechanisms underlying the impaired contractility of diabetic cardiomyopathy. World J. Cardiol. 6: 577–584. 2014.
18. *Dallak M., Al-Ani B., Kader D.H.A., Eid R.A., Haidara M.A.* Insulin suppresses type 1 Diabetes Mellitus–induced ventricular cardiomyocyte damage associated with the inhibition of biomarkers of inflammation and oxidative stress in rats. Pharmacology. 104: 157–165. 2019.
19. *Jourdon P., Feuvray D.* Calcium and potassium currents in ventricular myocytes isolated from diabetic rats. J. Physiol. (Lond). 470: 411–429. 1993.
20. *Shimoni Y., Ewart H.S., Severson D.* Type I and II models of diabetes produce different modifications of K currents in rat heart: role of insulin. J. Physiol. 507: 485–496. 1998.
21. *Shimoni Y., Ewart H.S., Severson D.* Insulin stimulation of rat ventricular K^+ currents depends on the integrity of the cytoskeleton. J. Physiol. 514: 735–745. 1999.
22. *Casis O., Gallego M., Iriarte M., Sµnchez-Chapula J.A.* Effects of diabetic cardiomyopathy on regional electrophysiologic characteristics of rat ventricle. Diabetologia. 43: 101–109. 2000.
23. *Nygren A., Olson M.L., Chen K.Y., Emmett T., Kargacin G., Shimoni Y.* Propagation of the cardiac impulse in the diabetic rat heart: reduced conduction reserve. J. Physiol. 580: 543–560. 2007.

24. *Dobretsov M., Backonja M.M., Romanovsky D., Stimers J.R.* Animal models of diabetic neuropathic pain. In: *Ma C., Zhang J. M.* (eds) Animal models of pain. Neuromethods. V. 49. Humana Press. Totowa. NJ. 147–169. 2011.
25. *Kubasov I.V., Stepanov A., Bobkov D., Radwanski P.B., Terpilowski T.A., Dobretsov M., Gyorke S.* Sub-cellular electrical heterogeneity revealed by loose patch recording reflects differential localization of sarcolemmal ion channels in intact rat hearts. Front. Physiol. 9: 61. 2018.
26. *Кубасов И.В., Бобков Д.Е.* Оптические и электрические ответы кардиомиоцитов в изолированном сердце крысы при развитии гипоксии. Рос. физиол. журн. им. И.М. Сеченова. 104(6): 670–675. 2018. [*Kubasov I.V., Bobkov D.E.* Optical and electrical responses of cardiomyocytes in isolated rat heart during development of hypoxia. Russ. J. Physiol. 104(6): 670–675. 2018. (In Russ)].
27. *Bub G., Camelliti P., Bollensdorff C., Stuckey D.J., Picton G., Burton R.A., Clarke K., Kohl P.* Measurement and analysis of sarcomere length in rat cardiomyocytes in situ and in vitro. Am. J. Physiol. Heart Circ. Physiol. 298: H1616–H1625. 2010.
28. *Moench I., Meekhof K.E., Cheng L.F., Lopatin A.N.* Resolution of hypo-osmotic stress in isolated mouse ventricular myocytes causes sealing of t-tubules. Exp. Physiol. 98: 1164–1177. 2013.
29. *Ferrantini C., Coppini R., Sacconi L., Tosi B., Zhang M. L., Wang G. L., de Vries E., Hoppenbrouwers E., Pavone F., Cerbai E., Tesi C., Poggesi C., Henk E.D.J.ter Keurs.* Impact of detubulation on force and kinetics of cardiac muscle contraction. J. Gen. Physiol. 143: 783–797. 2014.
30. *Romanovsky D., Wang J., Al-Chaer E.D., Stimers J.R., Dobretsov M.* Comparison of metabolic and neuropathy profiles of rats with streptozotocin-induced overt and moderate insulinopenia. Neuroscience. 170: 337–347. 2010.
31. *Hosokawa M., Dolci W., Thorens B.* Differential sensitivity of GLUT1- and GLUT2-expressing β cells to streptozotocin. Biochem. Biophys. Res. Com. 289: 1114–1117. 2001.
32. *Szablewski L.* Glucose transporters in healthy heart and in cardiac disease Int. J. Cardiol. 230: 70–75. 2017.
33. *Dobretsov M., Romanovsky D., Stimers J.R.* Early diabetic neuropathy: Triggers and mechanisms. World J. Gastroenterol. 13(2): 175–191. 2007.

TO CITE THIS ARTICLE:

Kubasov I.V., Bobkov D.E., Stepanov A.V., Sukhov I.B., Chistyakova O.V., Dobretsov M.G. Evaluation of the T-System of Rat Cardiomyocytes during Early Stages of Streptozotocin-Induced Diabetes. Russian Journal of Physiology. 106(9): 1098—1108.

DOI: 10.31857/S0869813920090046